Protein Science (2000), *9*:956–963. Cambridge University Press. Printed in the USA.

Crystal structure of the antibiotic albomycin in complex with the outer membrane transporter FhuA

ANDREW D. FERGUSON,[1,2] VOLKMAR BRAUN,[3] HANS-PETER FIEDLER,[4]
JAMES W. COULTON,[1] KAY DIEDERICHS,[2] AND WOLFRAM WELTE[2]

[1]Fachbereich Biologie, Universität Konstanz, M656, Postfach 55 60, D-78457 Konstanz, Germany
[2]Department of Microbiology and Immunology, McGill University, 3775 University Street, Montreal, Quebec H3A 2B4, Canada
[3]Lehrstuhl Mikrobiologie/Membranphysiologie, Universität Tübingen, Auf der Morgenstelle 28, D-72076 Tübingen, Germany
[4]Lehrstuhl Mikrobiologie/Biotechnologie, Universität Tübingen, Auf der Morgenstelle 28, D-72076 Tübingen, Germany

(RECEIVED January 3, 2000; FINAL REVISION March 21, 2000; ACCEPTED March 30, 2000)

Abstract

One alternative method for drug delivery involves the use of siderophore-antibiotic conjugates. These compounds represent a specific means by which potent antimicrobial agents, covalently linked to iron-chelating siderophores, can be actively transported across the outer membrane of Gram-negative bacteria. These "Trojan Horse" antibiotics may prove useful as an efficient means to combat multi-drug–resistant bacterial infections. Here we present the crystallographic structures of the natural siderophore-antibiotic conjugate albomycin and the siderophore phenylferricrocin, in complex with the active outer membrane transporter FhuA from *Escherichia coli*. To our knowledge, this represents the first structure of an antibiotic bound to its cognate transporter. Albomycins are broad-host range antibiotics that consist of a hydroxamate-type iron-chelating siderophore, and an antibiotically active, thioribosyl pyrimidine moiety. As observed with other hydroxamate-type siderophores, the three-dimensional structure of albomycin reveals an identical coordination geometry surrounding the ferric iron atom. Unexpectedly, this antibiotic assumes two conformational isomers in the binding site of FhuA, an extended and a compact form. The structural information derived from this study provides novel insights into the diverse array of antibiotic moieties that can be linked to the distal portion of iron-chelating siderophores and offers a structural platform for the rational design of hydroxamate-type siderophore-antibiotic conjugates.

Keywords: albomycin; antibiotic; FhuA; rational drug design; siderophore-antibiotic conjugate; TonB-dependent outer membrane transporter

Bacterial virulence is often related to an organism's ability to compete for essential nutrients (Martinez et al., 1990). The virtual insolubility of ferric iron under oxygen-rich conditions severely restricts bacterial growth. To satisfy their iron requirement, most bacteria have evolved a diverse series of high-affinity iron acquisition systems that are dependent upon the synthesis and/or uptake of low molecular weight iron chelators termed siderophores (Neilands, 1995; Braun et al., 1998). Transporters bind these iron chelates with high affinity and mediate their uptake across the outer membrane of Gram-negative bacteria with an energy-dependent mechanism of transport. The energy required to translocate these compounds is derived from the proton motive force of the cytoplasmic membrane as transduced by the TonB-ExbB-ExbD complex (Braun, 1995).

The diverse range of siderophores that are transported by TonB-dependent transport systems can be exploited to develop novel strategies for drug delivery. The concept that siderophore analogues, termed siderophore-antibiotic conjugates, can be actively transported across the bacterial cell envelope is well established (Roosenberg et al., 2000). Albomycins are "natural" iron-chelating siderophores of fungal origin that display broad-spectrum bactericidal activity against both Gram-positive and Gram-negative bacteria (Knüsel & Zimmermann, 1975). The following bacterial strains have been shown to be sensitive to albomycin: *Escherichia coli*, *Staphylococcus aureus*, and other Staphylococci, *Bacillus subtilis*, *Klebsiella pneumoniae*, *Streptococcus pneumoniae*, *Salmonella* species, *Bordetella pertussis*, and *Spirochaeta* species. In contrast, *Listeria*, *Mycobacterium tuberculosis*, and *Bacillus mycoides* are albomycin-resistant (Nüesch & Knüsel, 1967). The exquisite inhibitory activity of albomycins (minimal inhibitory concentration of 0.005 μg/mL, compared to 0.1 μg/mL for ampicillin; Pugsley et al., 1987) depends upon their ability to utilize the ferric hydroxamate uptake system for their uptake across both the outer and cytoplasmic membranes. Albomycin, a structural analogue of the fungal siderophore ferrichrome, is actively transported across the outer membrane of *E. coli* by FhuA. Once translocated into the

Reprint requests to: Wolfram Welte, Fachbereich Biologie, Universität Konstanz, M656, D-78457 Konstanz, Germany; e-mail: wolfram.welte@uni-konstanz.de.

periplasm, the antibiotic is bound by the periplasmic binding protein FhuD (Rohrbach et al., 1995), shuttled to an ABC transporter embedded within the cytoplasmic membrane (FhuBC), and actively transported into the cytoplasm (Schultz-Hauser et al., 1992). Bacterial mutants with deletions in any one of the *fhuABCD* genes are unable to transport albomycin across the cell envelope and thus are resistant to its antimicrobial effects (Kadner et al., 1980).

Similar to ferrichrome and its structural analogues, ferricrocin and phenylferricrocin, the iron-chelating component of albomycin is a tri-*δ*-*N*-hydroxy-*δ*-*N*-acetyl-L-ornithine peptide. Covalently linked to the iron-binding component of albomycin, by a short amino acetyl linker, is a thioribosyl pyrimidine antibiotic group (Hartmann et al., 1979). The chemical structures (Benz et al., 1982) and the thioribosyl pyrimidine substituent conformations in aqueous solution (Benz et al., 1984) of three albomycin subtypes (δ_1, δ_2, and ϵ) synthesized by *Streptomyces spec* strain WS116 have been determined. Substitution of the thioribosyl moiety with a ribosyl analogue abolishes the antimicrobial activity of δ_1-albomycin (Paulsen et al., 1987). In *E. coli*, enzymatic cleavage of the antibiotic group from the iron-chelating portion of albomycin is accomplished by peptidase N. Bacterial mutants devoid of peptidase N activity are albomycin-resistant, indicating that peptidase-mediated cleavage is essential for albomycin to exert its bactericidal activity (Braun et al., 1983). Although the transport and activation pathways of albomycin are known, the intracellular target remains to be determined. The absence of albomycin-resistant target site mutants suggests that albomycin interferes with critical bacterial cell functions or has multiple intracellular targets.

Results and discussion

We have determined the three-dimensional structures of FhuA in complex with phenylferricrocin and albomycin at 2.95 and 3.10 Å resolution, respectively (Fig. 1; Table 1). The structures of unliganded FhuA and FhuA in complex with ferricrocin (Ferguson et al., 1998b) and ferrichrome (Locher et al., 1998) are also available. These crystallographic structures show that FhuA is organized into two domains (Fig. 2A). The elliptical-shaped β-barrel domain is formed by 22 antiparallel transmembrane β-strands. The cork domain, consisting of a mixed four-stranded β-sheet and a series of short α-helices, fills the barrel interior. The presence of the cork domain delineates a pair of pockets within FhuA. The larger extracellular pocket is open to the external medium while the smaller periplasmic pocket is in contact with the periplasm. The interior walls of the extracellular pocket, extracellular loops, and strands of the barrel domain are lined with aromatic residues (Fig. 2B). Hydroxamate-type siderophores, such as phenylferricrocin and albomycin, are polar but uncharged at physiological pH and are not inherently hydrophobic. The aromatic side-chain residues that line the inner walls of the extracellular pocket may function to extract the siderophore from the external medium.

Located within the extracellular pocket of FhuA, above the external outer membrane interface, is a single ligand molecule (Fig. 2A,B). The iron-chelating components of phenylferricrocin and albomycin are bound to FhuA in the same orientation and by the same side-chain residues (Fig. 2B) as previously observed with ferricrocin (Ferguson et al., 1998b) and ferrichrome (Locher et al., 1998). Residues from the extracellular pocket, apices A (Arg81), B (Gln100), and C (Tyr116) of the cork domain and from the barrel domain, form hydrogen bonds or van der Waals contacts with the phenylferricrocin (Figs. 3A, 4A; Table 2) or albomycin molecule (Figs. 3B,C, 4B; Table 3).

Due to inherent flexibility of the amino acetyl linker connecting the iron-chelating moiety of albomycin to the thioribosyl pyrimidine substituent, two albomycin conformations, an extended and a compact conformational isomer, have been identified in the binding site of FhuA. These transport-active albomycin conformations may only represent a small portion of a larger set of conformations that exist in aqueous solution. The extended conformational isomer extends upward into the extracellular loops of FhuA, while the compact conformational isomer fills part of the lower portion of the extracellular pocket. Side-chain residues from the extracellular

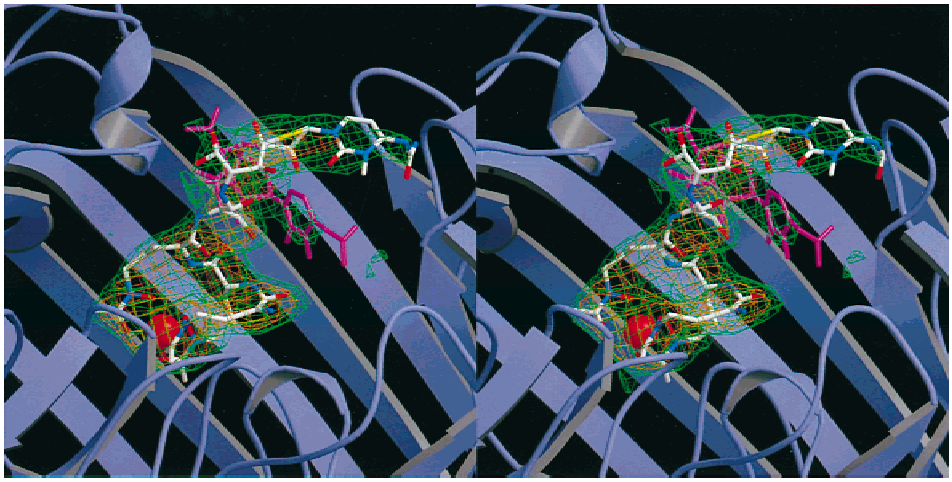

Fig. 1. Representative electron density section of the FhuA-albomycin complex. Stereoview of the final $3F_{obs} - 2F_{calc}$ electron density map contoured at 2σ (orange) and 1σ (green) at a resolution of 3.10 Å showing the albomycin-binding site. Both conformational isomers of the albomycin molecule are presented. The extended conformational isomer is shown with carbon atoms, white; oxygen atoms, red; nitrogen atoms, blue; and sulfur atoms, yellow. The thioribosyl pyrimidine group of the compact conformational isomer is colored purple. The ferric iron atom is shown as a large red sphere.

Table 1. *Crystallographic data*[a]

	FhuA in complex with phenylferricrocin	FhuA in complex with albomycin
Data collection and reduction		
Space group	$P6_1$	$P6_1$
Unit cell		
a (Å)	172.10	171.90
b (Å)	172.10	171.90
c (Å)	87.65	87.55
Number of molecules per asymmetric unit	1	1
Number of measured reflections	231,385	197,612
Number of unique reflections	31,400	38,021
Completeness (%)	94.8 (82.0)	94.9 (94.3)
Resolution (Å)	2.95	3.10
R_{sym} (%)	6.4 (22.0)	13.9 (34.9)
R_{meas} (%)	6.8 (25.8)	15.0 (40.2)
$R_{merge\text{-}F}$ (%)	6.5 (29.1)	15.3 (36.1)
I/σ	19.6 (3.8)	6.16 (2.2)
Structural refinement		
R_{cryst} (%)	22.5	22.2
R_{free} (%)	27.8	28.3
RMSD		
Bond lengths (Å)	0.008	0.020
Bond angles (deg)	1.8	2.3
Dihedral angles (deg)	26.2	25.8
Improper angles (deg)	0.88	2.82

[a]All X-ray diffraction data were collected at Max-Lab II beam line I711 (Lund, Sweden) at a temperature of 100 K using a wavelength of 1.051 Å. Brackets indicate the highest resolution shell.

pocket, extracellular loops, and strands of the barrel domain form numerous hydrogen bonds and van der Waals contacts with both conformational isomers (Figs. 3B,C, 4B; Table 3). In accord with the composition of the ligand binding sites, deletion of residues 236–248 (Killmann et al., 1998) or insertion of a tetrapeptide after residue 241 (Koebnik & Braun, 1993) inhibits ferrichrome and albomycin transport. Furthermore, preincubation of ferricrocin with bacterial cells expressing the wild-type receptor inhibits cell killing by albomycin (Pugsley et al., 1987). These liganded complexes of FhuA provide a structural explanation for the competitive binding of albomycin and ferricrocin to the binding site of the transporter.

Table 2. *FhuA-phenylferricrocin interactions*[a]

Residue atom	Location	Distance (Å)	Type of interaction
Arg81-NH1	Apex A	2.8	Hydrogen bond with the O8 atom
Arg81-NH2	Apex A	2.7	Hydrogen bond with O3 atom
Tyr87-CE2	Coil region of the cork domain	3.9	van der Waals contact with C35 atom
Gly99-N	Apex B	3.6	Electrostatic interactions with O17 atom
Gln100-CG	Apex B	3.1	van der Waals contact with C37 atom
Phe115-CD1	Apex C	3.9	van der Waals contact with the C27 atom
Tyr116-OH	Apex C	2.8	Hydrogen bond with O10 atom
Tyr244-OH	L3	2.7	Hydrogen bond with O6 atom
Trp246-NE1	L3	3.1	Hydrogen bond with O3 atom
Tyr313-CZ	β7	3.5	van der Waals contact with C25 atom
Tyr315-OH	L4	3.2	Hydrogen bond with O1 atom
Phe391-CE2	β9	3.5	van der Waals contact with O4 atom
Phe693-CE1	L11	3.8	van der Waals contact with C34 atom

[a]Listed are the residue atom, location, distance, and type of interaction formed between all FhuA side-chain residues within 4 Å of phenylferricrocin atoms. See Figure 2A for further details of the hydrogen bonding pattern and electrostatic interactions between FhuA and phenylferricrocin.

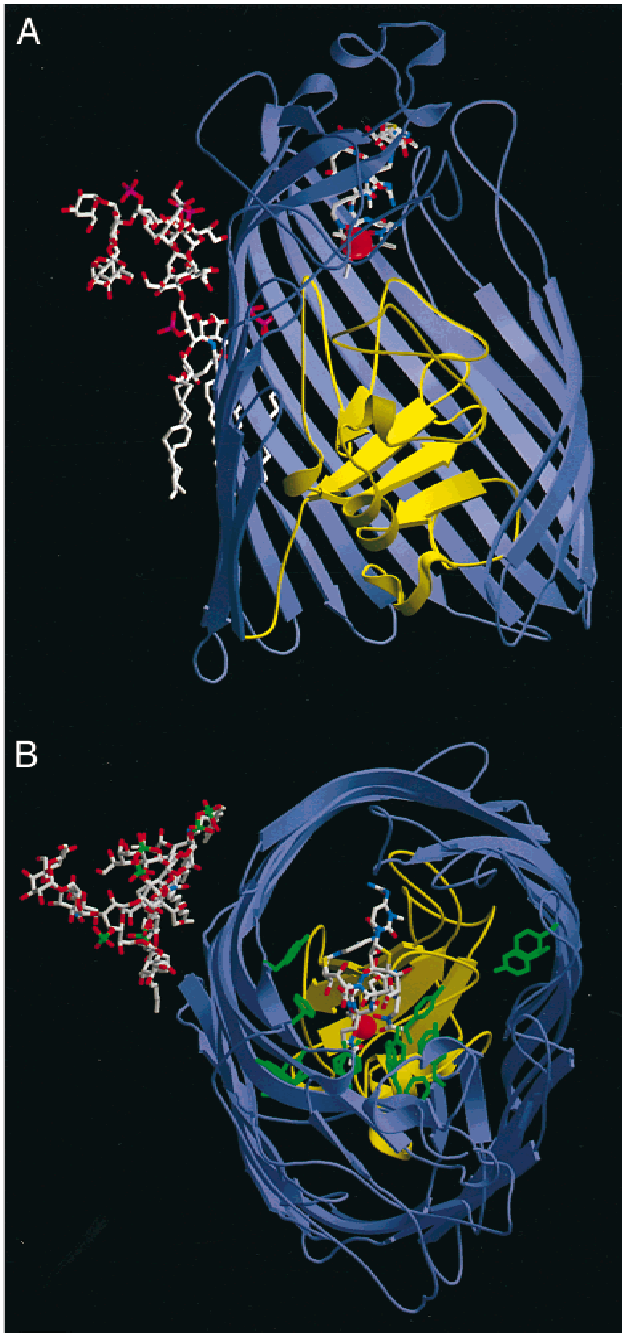

Fig. 2. The FhuA–albomycin–lipopolysaccharide complex. **A:** General description of the complex. The view is perpendicular to the barrel axis. Those strands, which form the front of the barrel domain, have been removed to provide an unobstructed view of the cork domain. **B:** The external aromatic cavity of the complex as viewed from the external environment. Those side-chain residues (Tyr244, Trp246, Tyr275, Tyr313, Tyr315, Tyr325, Tyr345, Trp379, Phe391, Phe410, Phe412, Tyr423, Phe513, Phe558, Tyr595, Tyr601, Phe650, Phe693, Tyr696, and Phe699), which compose the external aromatic cavity, are colored green. In both panels, the barrel domain and the cork domain are colored blue and yellow, respectively. The extended δ_2-albomycin conformational isomer and the lipopolysaccharide molecule are shown as a bond model with carbon atoms, white; sulfur atoms, yellow; oxygen atoms, red; and nitrogen atoms, blue. The ferric iron atom is shown as a large red sphere.

Structural alignment of the α-carbon coordinates of FhuA and its liganded complexes reveals near perfect superposition (root-mean-square deviation (RMSD) of 0.25 Å) of the barrel domains. However, two distinct conformations, unliganded and liganded, are observed in the cork domain. Upon ligand binding to FhuA, an upward translation (1–2 Å) of apices A and B, and other residues of the cork domain, is observed. This movement is propagated to the periplasmic pocket of FhuA, promoting the unwinding of an amino proximal α-helix designated the switch helix (Ferguson et al., 1998b; Locher et al., 1998). The structures of FhuA complexed with ferrichrome, ferricrocin, phenylferricrocin, and albomycin are virtually identical with regard to the protein and the bound iron-chelating component of the ligand. This conservation of the allosteric transition suggests that all liganded complexes promote FhuA's interaction with TonB, which is presumably mediated by the TonB-box of the transporter (Moeck & Coulton, 1998).

Early investigations into the application of siderophore-antibiotic conjugates as antimicrobial agents were provided by Zähner et al. (1977). In this study, a series of ferricrocin and ferroxamine B-based siderophore-antibiotic conjugates were synthesized, and their antimicrobial activities assessed. These early studies have been amplified by the synthesis of a large variety of hydroxamate and catechol-type siderophore-antibiotic conjugates. Many of these compounds display strong antimicrobial activity and are actively transported across the outer membrane by TonB-dependent receptors (Diarra et al., 1996; Ghosh et al., 1996). However, the loss of specific outer membrane transporters may facilitate the development of resistance to certain classes of structurally related siderophore-antibiotic conjugates (Brochu et al., 1992; Minnick et al., 1992; Diarra et al., 1996). Resistance to these agents could be minimized by developing siderophore-antibiotics conjugates that target more than one TonB-dependent receptor, which function both as transporters and bacterial virulence factors (Roosenberg et al., 2000). Moreover, spontaneous *tonB* mutations would severely restrict bacterial growth in vivo, as all TonB-dependent activity would be disrupted.

Siderophore-antibiotic conjugates consist of three parts: an iron-chelating siderophore, a peptide linker, and an antibiotic group. The principal requirement in the design of these compounds is that the siderophore must be recognized and thereby transported across the outer membrane. The available liganded complexes provide the structural basis for ligand recognition by FhuA. Most hydrogen bonds and van der Waals contacts are formed between the iron-chelating component of the siderophore and characteristic side-chain residues from apices A, B, and C of the cork domain, and the extracellular loops and strands of the barrel domain. The structural composition of the binding site surrounding the iron-chelating component of the siderophore is spatially restrictive, demonstrating that recognition of hydroxamate-type siderophore analogues by FhuA is based primarily on the conformation of the iron-chelating component. It has been shown that chemical or conformational alteration of this portion of the siderophore abrogates receptor-specific recognition (Jurkevitch et al., 1992). The remaining portions of the siderophore are bound less tightly, with few apparent constraints on the chemical structure, conformation, or the spatial requirements of the linker or the antibiotic substituent. Furthermore, the size of the extracellular pocket of FhuA has the potential to accommodate larger siderophore-antibiotic conjugates.

The tolerant constraints imposed upon the binding of hydroxamate-type siderophore analogues may also apply to ligand trans-

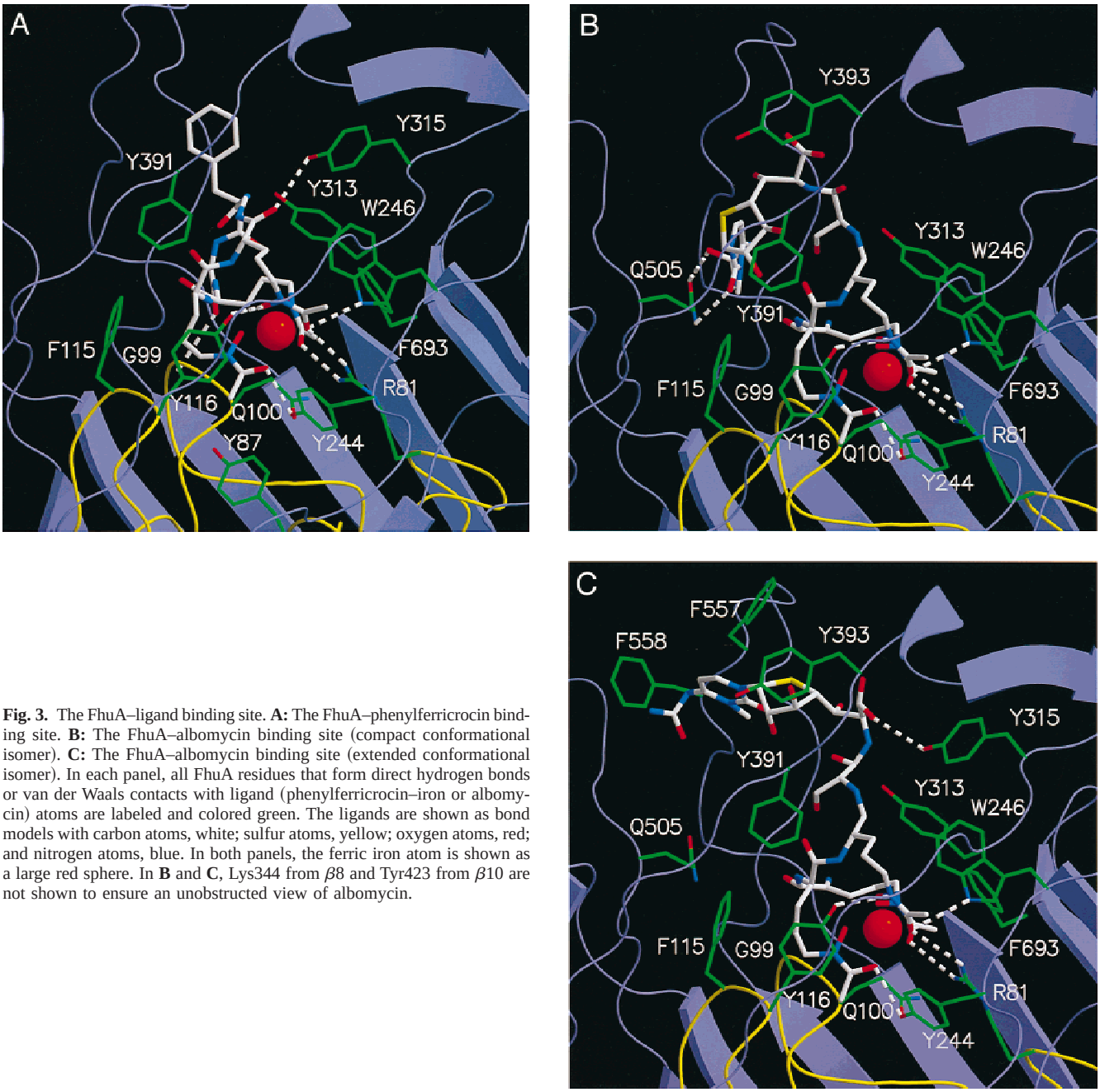

Fig. 3. The FhuA–ligand binding site. **A:** The FhuA–phenylferricrocin binding site. **B:** The FhuA–albomycin binding site (compact conformational isomer). **C:** The FhuA–albomycin binding site (extended conformational isomer). In each panel, all FhuA residues that form direct hydrogen bonds or van der Waals contacts with ligand (phenylferricrocin–iron or albomycin) atoms are labeled and colored green. The ligands are shown as bond models with carbon atoms, white; sulfur atoms, yellow; oxygen atoms, red; and nitrogen atoms, blue. In both panels, the ferric iron atom is shown as a large red sphere. In **B** and **C**, Lys344 from β8 and Tyr423 from β10 are not shown to ensure an unobstructed view of albomycin.

port. The precise transport mechanism has not been elucidated. However, according to our proposal (Ferguson et al., 1998b), formation of the FhuA–TonB complex induces conformational changes in the cork domain, which disrupt the high-affinity ligand-binding site, and thus promote the release of the ligand from its binding site. This event is followed or accompanied by the formation of a channel located between the inner barrel wall and the cork domain termed the putative channel-forming segment. These tolerant binding constraints are in accord with this proposed transport mechanism (Ferguson et al., 1998b). Moreover, the fact that active transport is mediated by FhuA and the FhuBCD proteins suggests that both transporters may recognize the iron-chelating component of hydroxamate-type siderophores and their analogues. In conclusion, these results provide a structural basis for the design of hydroxamate-type siderophore-antibiotic conjugates. Using rational modular design, a large variety of designer antibiotics may be chemically synthesized by combining compatible iron-chelating siderophores, peptide linkers, and potent antibiotic groups. By utilizing specific siderophore receptors for their transport across the cell envelope, antimicrobial agents of this type may selectively target and ultimately kill bacteria.

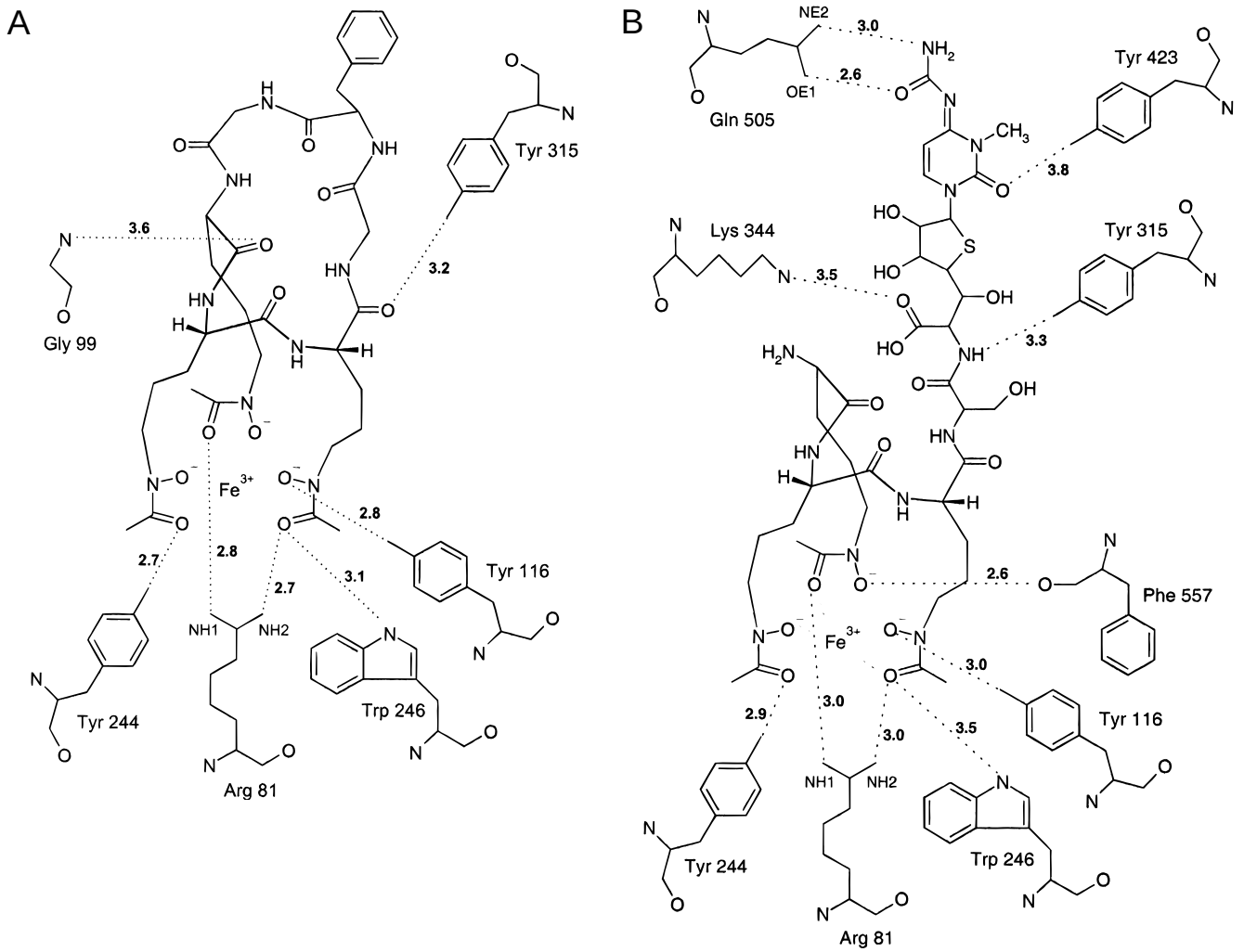

Fig. 4. Schematic comparison of the hydrogen bonding pattern and electrostatic interactions of (**A**) phenylferricrocin and (**B**) albomycin (extended conformational isomer) with FhuA side-chain residues in the ligand binding site. The chemical structures of phenylferricrocin and albomycin are shown with hydrogen bonds and charge interactions indicated as dotted lines (distances are given in Å). See Table 2 (phenylferricrocin) and Table 3 (albomycin) for additional van der Waals contacts.

Materials and methods

Protein expression, purification, and crystallization

A recombinant FhuA protein was constructed by inserting a hexahistidine tag plus five additional linker residues (SSHHHHHHGSS) into the *fhuA* gene after residue 405 (Moeck et al., 1994, 1996). FhuA was expressed and purified as previously described (Ferguson et al., 1998a, 1998b). δ_2-Albomycin (albomycin) was purified from *Streptomyces griseus* strain TÜ 6 as previously described (Fiedler et al., 1985). FhuA was cocrystallized with albomycin and phenylferricrocin and one LPS molecule using a final ligand concentration of 0.3 mM. Crystals of FhuA were grown using the hanging drop vapor diffusion technique by mixing equal volumes (5 μL) of FhuA [10 mg/mL, 0.80% *N,N*-dimethyldecylamine-*N*-oxide and 10 mM ammonium acetate (pH 8.0)] and reservoir solution [12% polyethylene glycol (PEG) 2,000 monomethyl ether, 0.1 M sodium cacodylate (pH 6.4), 20% glycerol, 3% PEG 200, and 1% *cis*-inositol]. Crystals grew within seven days to a final size of 200 × 200 × 200 μm^3 at 18 °C. All crystals were mounted in cryoloops and flash frozen by direct immersion in liquid nitrogen.

Crystallographic data collection, structure determination, and refinement

All X-ray diffraction data were collected at 100 K using a cryostream apparatus with synchrotron radiation at beam line I711, Max Lab-II (Table 1). X-ray diffraction data were processed and reduced using the program XDS (Kabsch, 1988). Initial phases for both FhuA complexes were calculated using the FhuA–ferricrocin coordinates (1qff.pdb) as an initial model. Structural models for both FhuA–ligand complexes were built into an experimental electron density map using the program O (Jones et al., 1991). Both models were refined with the program CNS using molecular dynamics and the maximum likelihood target (Brünger et al., 1998). Following rounds of model building and structural refinement the

Table 3. *FhuA–albomycin interactions*[a]

Residue atom	Location	Distance (Å)	Type of interaction
Arg81-NH1*†	Apex A	3.0	Hydrogen bond with the O5 atom
Arg81-NH2*†	Apex A	3.1	Hydrogen bond with O1 atom
Gly99-O*†	Apex B	3.7	van der Waals contact with C13 atom
Gln100-O*†	Apex B	3.7	van der Waals contact with C18 atom
Phe115-CZ*	Apex C	3.7	van der Waals contact with the O17 atom
Tyr116-OH*†	Apex C	3.0	Hydrogen bond with N3 atom
Tyr244-OH*†	L3	2.9	Hydrogen bond with O3 atom
Trp246-NE1*†	L3	3.5	Hydrogen bond with O1 atom
Tyr313-OH*†	β7	3.5	van der Waals contact with C9 atom
Tyr315-OH†	L4	3.1	Hydrogen bond with the O12 atom
Lys344-NZ†	β9	3.7	Electrostatic interactions with the O12 atom
Phe391-CG*	β9	3.0	van der Waals contact with O18 atom
Phe391-CD2†	β9	3.9	van der Waals contact with C12 atom
Tyr393-CD1*	L5	3.2	van der Waals contact with O12 atom
Tyr393-CD1†	L5	3.5	van der Waals contact with O12 atom
Tyr423-OH*	β10	3.7	Electrostatic interactions with O15 atom
Gln505-OE1*	L7	2.7	Hydrogen bond with O16 atom
Gln505-NE2*	L7	3.0	Hydrogen bond with N10 atom
Phe557-O†	β15	2.8	Hydrogen bond with N11 atom
Phe558-CE1†	β15	3.0	van der Waals contact with N10 atom
Phe693-CE2*†	L11	3.5	van der Waals contact with C20 atom

[a]Listed are the residue atom, location, distance, and type of interaction formed between all FhuA side-chain residues within 4 Å of albomycin atoms. Those interactions that are specific to the compact albomycin conformational isomer are marked with an asterisk (*); those that are specific for the extended albomycin conformational isomer are denoted with a dagger (†). See Figure 2B for further details of the hydrogen bonding pattern and electrostatic interactions between FhuA and albomycin.

final models contain residues 19–714, one lipopolysaccharide molecule, one ligand molecule (albomycin or phenylferricrocin), and 332 and 299 water molecules for the FhuA–albomycin and FhuA–phenylferricrocin models, respectively. The lipopolysaccharide molecule is noncovalently bound to the membrane-embedded surface of FhuA and forms electrostatic and van der Waals contacts with side-chain residues from β7 through β11.

Figures

All color figures were prepared using MOLSCRIPT (Kraulis, 1991) and Raster3D (Merrit & Bacon, 1997). Figure 4 was prepared with the program ISIS Draw.

Protein Data Bank accession codes

Both sets of crystallographic coordinates have been deposited in the Protein Data Bank with the following accession codes: 1qkc (FhuA in complex with albomycin) and 1qjq (FhuA in complex with phenylferricrocin).

Acknowledgments

We gratefully acknowledge A. Svensson at Max-Lab II (beam line I711) for his assistance during data collection and J. Ködding for figure preparation. This work is supported by the Deutsche Forschungsgemeinschaft (to V.B. and W.W.), and by the Natural Sciences and Engineering Research Council, Canada (to J.W.C.). A.D.F. is the recipient of a Deutscher Akademischer Austauschdienst Grant for Study and Research and a Medical Research Council of Canada Doctoral Research Award.

References

Benz G, Born L, Brieden M, Grosser R, Kurz J, Paulsen H, Sinnwell V, Weber B. 1984. Absolute Konfiguration der Desferriform der Albomycine. *Liebigs Ann Chem* 1408–1423.

Benz G, Schröder T, Kurz J, Wünsche C, Karl W, Steffens G, Pfitzner J, Schmidt D. 1982. Konstitution der Desferriform der Albomycine δ_1, δ_2, ϵ. *Angew Chem Suppl* 1322–1335.

Braun V. 1995. Energy-coupled transport and signal transduction through the Gram-negative outer membrane via TonB-ExbB-ExbD-dependent receptor proteins. *FEMS Microbiol Rev 16*:295–307.

Braun V, Günther K, Hantke K, Zimmermann L. 1983. Intracellular activation of albomycin in *Escherichia coli* and *Salmonella typhimurium*. *J Bacteriol 156*:308–315.

Braun V, Hantke K, Köster W. 1998. Iron transport and storage in microorganisms, plants, and animals. In: Siegel A, Siegel H, eds. *Metal ions in biological systems*. New York: Marcel Dekker. pp 67–145.

Brochu A, Brochu N, Nicas T, Parr TR Jr, Minnick AA Jr, Dolence EK, McKee JA, Miller MJ, Lavoie MC, Malouin F. 1992. Modes of action and inhibitory activities of new siderophore-β-lactam conjugates that use specific iron uptake pathways for entry into bacteria. *Antimicrob Agents Chemother 36*:2166–2175.

Brünger AT, Adams PD, Clore GM, DeLano WL, Gros P, Grosse-Kunstleve RW, Jiang J-S, Kuszewski J, Nilges M, Pannu NS, et al. 1998. Crystallography & NMR system: A new software suite for macromolecular structure determination. *Acta Crystallogr D 54*:905–921.

Diarra MS, Lavoie MC, Jacques M, Darwish I, Dolence EK, Dolence JA, Ghosh A, Ghosh M, Miller MJ, Malouin F. 1996. Species selectivity of new siderophore-drug conjugates that use specific iron uptake for entry into bacteria. *Antimicrob Agents Chemother 40*:2610–2617.

Ferguson AD, Breed J, Diederichs K, Welte W, Coulton JW. 1998a. An internal affinity-tag for purification and crystallization of the siderophore receptor FhuA, integral outer membrane protein from *Escherichia coli* K-12. *Protein Sci 7*:1636–1638.

Ferguson AD, Hofmann E, Coulton JW, Diederichs K, Welte W. 1998b. Siderophore-mediated iron transport: Crystal structure of FhuA with bound lipopolysaccharide. *Science 282*:2215–2220.

Fiedler H-P, Walz F, Döhle A, Zähner H. 1985. Albomycin: Studies on fermentation, isolation and quantitative determination. *Appl Microbiol Biotechnol 21*:341–347.

Ghosh A, Ghosh M, Niu C, Malouin F, Moellmann U, Miller MJ. 1996. Iron transport-mediated drug delivery using mixed-ligand siderophore-β-lactam conjugates. *Chem Biol 3*:1011–1019.

Hartmann A, Fiedler H-P, Braun V. 1979. Uptake and conversion of the antibiotic albomycin by *Escherichia coli* K-12. *Eur J Biochem 99*:517–524.

Jones TA, Zou JY, Cowan SW, Kjeldgaard M. 1991. Improved methods for building protein models in electron density maps and the location of errors in these models. *Acta Crystallogr A 47*:110–119.

Jurkevitch E, Hadar Y, Chen Y, Libman J, Shanzer A. 1992. Iron uptake and molecular recognition in *Pseudomonas putida*: Receptor mapping with ferrichrome and its biomimetic analogs. *J Bacteriol 174*:78–83.

Kabsch W. 1988. Evaluation of single crystal X-ray diffraction data from a position sensitive detector. *J Appl Crystallogr 21*:916–924.

Kadner RJ, Heller K, Coulton JW, Braun V. 1980. Genetic control of hydroxamate-mediated iron uptake in *Escherichia coli. J Bacteriol 143*:256–264.

Killmann H, Herrmann C, Wolff H, Braun V. 1998. Identification of a new site for ferrichrome transport by comparison of the FhuA proteins of *Escherichia coli*, *Salmonella paratyphi* B, *Salmonella typhimurium* and *Pantoea agglomerans*. *J Bacteriol 180*:3845–3852.

Knüsel F, Zimmermann W. 1975. Sideromycins. In: Corcoran JW, Hahn FE, eds. *Antibiotics III. Mechanisms of action of antimicrobial and antitumor agents*. Heidelberg: Springer Verlag. pp 653–667.

Koebnik R, Braun V. 1993. Insertion derivatives containing segments of up to 16 amino acids identify surface- and periplasm-exposed regions of the FhuA outer membrane receptor of *Escherichia coli* K-12. *J Bacteriol 175*:826–839.

Kraulis PJ. 1991. MOLSCRIPT: A program to produce both detailed and schematic plots of protein structures. *J Appl Crystallogr 24*:946–950.

Locher KP, Rees B, Koebnik R, Mitschler A, Moulinier L, Rosenbusch J, Moras D. 1998. Transmembrane signaling across the ligand-gated FhuA receptor: Crystal structures of free and ferrichrome-bound states reveal allosteric changes. *Cell 95*:771–778.

Martinez JL, Delgado-Iribarren A, Baquero F. 1990. Mechanisms of iron acquisition and bacterial virulence. *FEMS Microbiol Rev 75*:45–56.

Merrit EA, Bacon DJ. 1997. Raster3D photorealistic molecular graphics. *Methods Enzymol 277*:505–524.

Minnick AA, McKee JA, Dolence EK, Miller MJ. 1992. Iron transport-mediated antibacterial activity of and development of resistance to hydroxamate and catechol siderophore-carbacephalosporin conjugates. *Antimicrob Agents Chemother 36*:840–850.

Moeck GS, Coulton JW. 1998. TonB-dependent iron acquisition: Mechanisms of siderophore-mediated active transport. *Mol Microbiol 128*:675–681.

Moeck GS, Fazly-Bazzaz BS, Gras MF, Ravi TS, Ratcliffe MJH, Coulton JW. 1994. Genetic insertion and exposure of a reporter epitope in the ferrichrome-iron receptor of *Escherichia coli* K-12. *J Bacteriol 176*:4250–4259.

Moeck GS, Tawa P, Xiang H, Ismail AA, Turnbull JL, Coulton JW. 1996. Ligand-induced conformational change in the ferrichrome-iron receptor of *Escherichia coli* K-12. *Mol Microbiol 22*:459–471.

Neilands JB. 1995. Siderophores: Structure and function of microbial iron transport compounds. *J Biol Chem 270*:26723–26726.

Nüesch J, Knüsel F. 1967. Sideromycines. In: Gottlieb P, Shaw PD, eds. *Antibiotics I: Mechanisms of action*. Berlin: Springer-Verlag. pp 449–541.

Paulsen H, Brieden M, Benz G. 1987. Synthese des Sauerstofanalogs der Desferriforn von δ_1-Albomycine. *Liebigs Ann Chem* 565–575.

Pugsley AP, Zimmerman W, Wehrli W. 1987. Highly efficient uptake of a rifamycin derivative via the FhuA-TonB-dependent uptake route in *Escherichia coli. J Gen Microbiol 133*:3505–3511.

Rohrbach MR, Braun V, Köster W. 1995. Ferrichrome transport in *Escherichia coli* K-12: Altered substrate specificity of mutated periplasmic FhuD and interactions of FhuD with the integral membrane protein FhuB. *J Bacteriol 177*:7186–7193.

Roosenberg JM, Lin Y-M, Lu Y, Miller MJ. 2000. Studies and syntheses of siderophores, microbial iron chelators, and analogs as potential drug delivery agents. *Curr Med Chem 7*:159–197.

Schultz-Hauser G, Köster W, Schwarz H, Braun V. 1992. Iron (III) hydroxamate transport in *Escherichia coli* K-12: FhuB-mediated membrane association of the FhuC protein and negative complementation of *fhuC* mutants. *J Bacteriol 174*:2305–2311.

Zähner H, Diddens H, Keller-Schierlein W, Nägeli H-U. 1977. Some experiments with semisynthetic sideromycins. *Jpn J Antibiot 30*:S201–S206.